Hindawi
Advances in Cell and Gene Therapy
Volume 2024, Article ID 1099113, 14 pages
https://doi.org/10.1155/2024/1099113

Research Article

Silencing of B4Galnt1 Gene Prevents GM2 Accumulation in Tay-Sachs Cells

Nurselin Ateş[1], **Orhan Kerim İnci**[1], **Seçil Akyıldız Demir**[2] and **Volkan Seyrantepe**[1,2]

[1]*Izmir Institute of Technology, Molecular Biology and Genetics Department, Gulbahce Campus, Urla, 35430 İzmir, Türkiye*
[2]*Izmir Institute of Technology, IYTEDEHAM, Gulbahce Campus, Urla, 35430 İzmir, Türkiye*

Correspondence should be addressed to Volkan Seyrantepe; volkanseyrantepe@iyte.edu.tr

Received 25 October 2023; Revised 29 February 2024; Accepted 6 March 2024; Published 26 March 2024

Academic Editor: Dao Pan

Introduction. The Tay-Sachs disease (TSD) is a progressive neurodegenerative disorder resulting from genetic mutations in the HEXA gene encoding the α-subunit of β-hexosaminidase A leading to the accumulation of GM2 ganglioside in the central nervous system. Multiple therapeutical strategies have been investigated such as gene therapy for Tay-Sachs patients; however, there is still no cure. In the present study, we suggest a new approach for the treatment of the Tay-Sachs disease with the concept of substrate reduction therapy by using AAV9-mediated RNAi technology targeting the *B4Galnt1* gene at the upstream of the enzymatic defect in TSD pathology to decrease GM2 biosynthesis and accumulation in cell models of TSD. *Material and Methods*. We employed AAV9-mediated shRNA transduction for mice and human Tay-Sachs cells. After transduction, expression levels of ganglioside metabolism genes were analyzed by RT-PCR and GM2 and lysosome-associated membrane protein 1 (LAMP1) protein levels were evaluated by immunocytochemistry analysis. *Results*. Here, we have shown that AAV9-shRNA transduction effectively reduced *B4Galnt1* expression in TSD cells demonstrating a reduction in GM2 accumulation and LAMP1. *Discussion*. Our data shows that AAV-mediated B4Galnt1-shRNA transduction can ameliorate disease pathologies by decreasing the lysosomal accumulation of GM2 through selectively reducing B4Gant1 activity in cell models of the Tay-Sachs disease. Therefore, we suggest promising novel experimental therapy for this devastating disease using a mouse model in the future.

1. Introduction

TSD is a subtype of rare, inherited metabolic disorders characterized by the accumulation of GM2 ganglioside particularly in the nervous system. Under normal circumstances, GM2 gangliosides are broken down by specific enzymes called β-hexosaminidase A in lysosomes [1]. Mutations in the Hexa gene in humans cause impairment in the degradation of GM2 ganglioside and result in progressive GM2 accumulation, especially in the central nervous system (CNS). Patients show clinically similar phenotypes, and the severity of the disease depends on the residual enzyme activity. Progressive neurological deterioration, motor dysfunction, vision and hearing impairment, seizures, feeding difficulties, and hypotonia are among the symptoms [2]. *Hexa*-/- mouse was previously generated as a model for TSD; however, it did not exhibit neuropathological symptoms that are observed in patients. Unlike humans in mice, a GA2-routed GM2 degradation pathway mediated by neuraminidase was suggested [3, 4]. Recently, the role of plasma membrane–associated neuraminidase Neu3 in glycolipid degradation in mice was investigated by generating *Hexa*-/-*Neu3*-/- double knock-out mouse model, and that model has been introduced as a novel valid murine model of TSD [5]. The *Hexa*-/-*Neu3*-/- mice were healthy at birth but died at nearly 5 months of age due to progressive neurodegeneration with neuronal loss,

Purkinje's cell depletion, and neuroinflammation. Neuroinflammation and neurological abnormalities such as slow movement, ataxia, and tremors were also reported in this mouse model [5, 6].

Gangliosides are the predominant glycosphingolipids found in neuronal cell membranes. Their distinctive surface patterns are formed through highly synchronized biosynthesis and degradation processes within secretory compartments (ER and Golgi) and endolysosomal systems, respectively. The ganglioside biosynthesis pathway involves the synthesis of ceramide backbone, sequential addition of sugar residues, sialylation, and the formation of complex gangliosides [7, 8]. This dynamic process requires the action of several enzymes like glycosyltransferases (i.e., B4Galnt1, GM3S, and GD3S), hexosaminidases (i.e., HexA and HexB), and neuraminidases (Neu1, Neu3, and Neu4). The GM2/GD2 synthase (also known as β-1,4-N–acetylgalactosaminyl transferase), encoded by the B4galnt1 gene, acts at a specific step in the pathway to create lactoseries gangliosides, which serve as intermediates for the generation of more complex gangliosides with additional sialic acid residues. The enzyme specifically catalyzes the transfer of N-acetylgalactosamine onto lactosylceramide, gangliosides GM3, and GD3, leading to the formation of sialic acid-containing gangliosides, GM2 and GD2 (Figure 1(a)) [9].

Gene therapy presents an appealing option for addressing lysosomal storage disorders (LSD) to reduce or reverse the accumulation of storage material in affected tissues due to its well-defined and broad range of therapeutic effectiveness [10, 11]. Various viral gene transfer vectors, like adenovirus, adeno-associated virus (AAV), lentivirus, and herpes virus, have been administered *in vitro* models or directly to the CNS of *in vivo* models of LSDs [10, 12]. Among viral delivery systems, AAV vectors possess several advantages, including robust *in vivo* expression of the therapeutic gene, minimal harmful effects, and the ability to activate the transgene in both actively dividing and resting cells [13]. AAV-mediated gene therapy has been used for the treatment of several LSDs such as mucopolysaccharidosis [14], Pompe's disease [15], Niemann-Pick's disease [16], GM1 gangliosidosis [17], and GM2 gangliosidosis [2, 18]. So far, researchers have employed various serotypes of AAV vectors and transgene cassettes to enhance brain and spinal cord transduction. Among these, AAV9 vectors demonstrated better transduction capabilities by their ability to cross the blood-brain barrier and transduce both neurons and glia [19], which has led to therapeutic strategies targeting various CNS diseases through intravascular AAV9-mediated gene delivery [20–22]. AAV9-mediated gene and/or substrate reduction therapy is efficacious for the treatment of LSDs [23, 24] and neurodegenerative diseases used in clinical applications [25, 26].

Multiple therapeutical strategies have been investigated like enzyme replacement therapy, pharmaceutical chaperone therapy, and hematopoietic stem cell replacement therapy for TSD; however, currently, there is no effective treatment available [27]. In the present study, we aimed to apply AAV9-shRNA-mediated substrate reduction therapy to prevent GM2 ganglioside accumulation in TSD cell models for the first time, and we investigated the impact of *in vitro* downregulation of *B4Galnt1* by using highly selective viral shRNA-mediated gene silencing.

2. Materials and Methods

2.1. Production of rAAV9-B4GALNT1-shRNA. Recombinant adeno-associated virus serotypes 9 (rAAV9) including shRNAs specific to human and mouse B4Galnt1 were prepared as follows. Human-specific rAAV9-H-B4GALNT1-shRNA and mouse-specific rAAV9-M-B4GALNT1-shRNA vectors were manufactured by VectorBuilder, and mCherry was used as reporter genes for shRNA constructs (Figure 1(b)). The sequences for the target regions of B4Galnt1 were as follows: human shRNA1, GTCAGGATCAAGGAGCAAGTA; human shRNA2, CAACTACAACTGGTCACTTAC; mouse shRNA1, CCTTGTTCCTTCCAGGATTAT; mouse shRNA2, GTCC CAAGTAACCACCAAATA; and mouse shRNA3, CCCAGT TCTGGATAAACTCAA. The locations of target regions for each shRNA were represented in the diagram (Figure 1(c)).

HEK293T cells were maintained in Dulbecco's Modified Eagle's Medium (DMEM), 10% fetal bovine serum (FBS), 2 mM L-glutamine, and 1% penicillin/streptomycin. Cells were plated 24 hours before transfection. 70–80% confluence cells were transfected with linear polyethyleneimine (Sigma-Aldrich) using a DNA mix for triple transfection: pAAV2/9n (Addgene), pAdDeltaF6 (Addgene), and pAAV9-B4Galnt1-shRNA at a ratio of 1 : 2 : 1. Polyethylenimine and DNA mix ratio was 3.5 : 1. At 72 h post-transfection, the cells containing rAAV9-mB4Galnt1-shRNA virus particles were harvested. After centrifugation at 500 g for 5 min, cells were frozen at -80°C for further analysis.

2.2. Quantitative PCR Analysis for Viral Copy Number Detection. Transfected HEK293T cells were resuspended in lysis buffer (150 mM NaCl, 50 mM Tris HCl, and pH 8.5). After freezing and thawing three times, they were centrifuged at 1,167 × g for 15 min at 4°C. rAAV9-mB4Galnt1-shRNA virus particles were collected in the supernatant. Viral media and cell supernatant were treated with DNase I (Life Technologies) to remove any residual DNA contaminants not present within the intact virus particles. DNase I was inactivated through the addition of 0.5 mM EDTA and incubation at 65°C for 10 min. Viral DNA was uncoated through digestion with proteinase K (Sigma-Aldrich) through incubation at 50°C for 60 min. The AAV virus capsids were disassembled, and the AAV vector genome was released into the solution. Proteinase K was then inactivated by incubation at 95°C for 20 min.

The number of viral genomes in each preparation was determined through quantitative real-time PCR with LightCycler 480 SYBR Green I Master Mix (Roche Life Science, Swiss) generating an amplicon from within the CMV promoter upstream of the mCherry transgene cassette: CMV forward (5′-TCATATGCCAAGTACGCCCC-3′) and CMV reverse (5′-CCCGTGAGTCAAACCGCTAT-3′). Samples were run on a LightCycler® 96 Instrument (Roche Life Science, Swiss). The conditions of PCR were as follows: 1 cycle of 10 min at 95°C and 45 cycles of 20 s at 95°C, 15 s at 61°C,

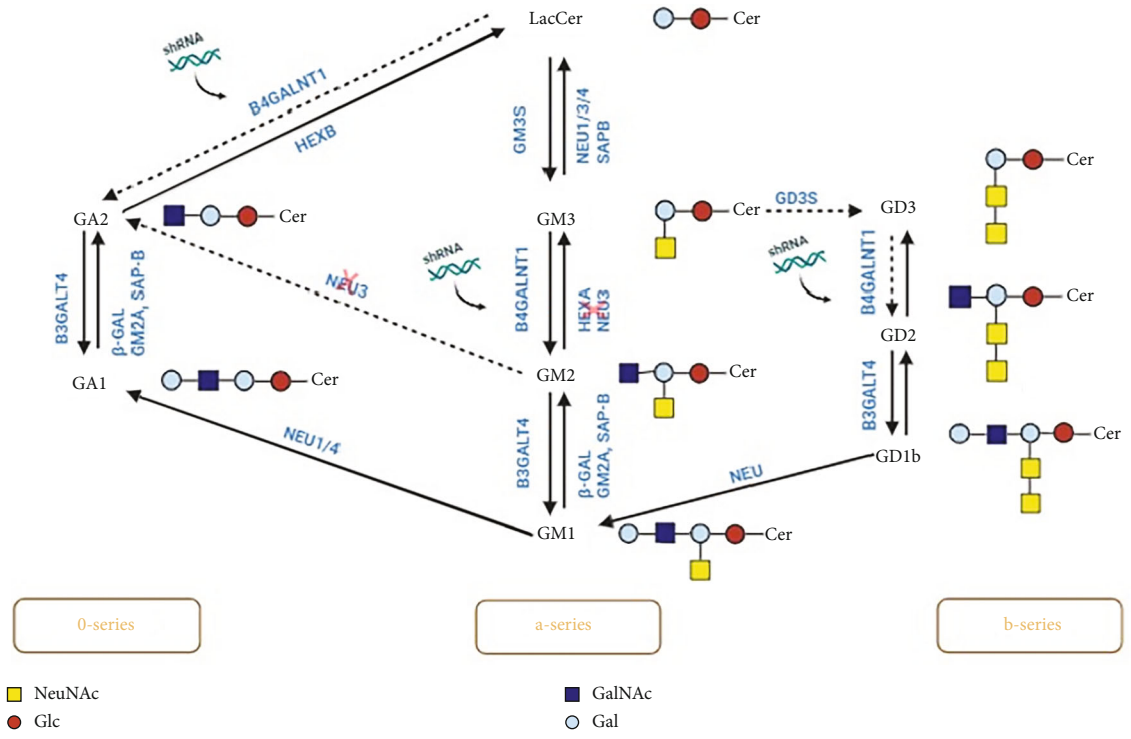

(a)

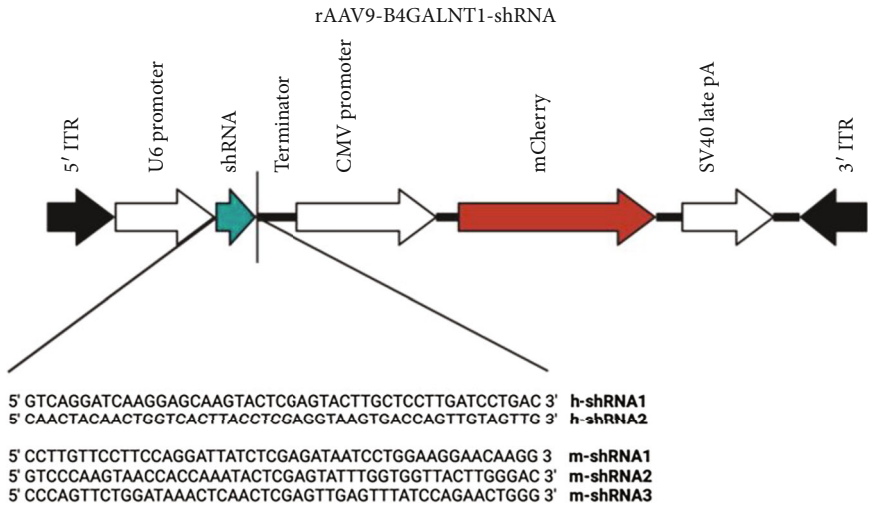

(b)

Figure 1: Continued.

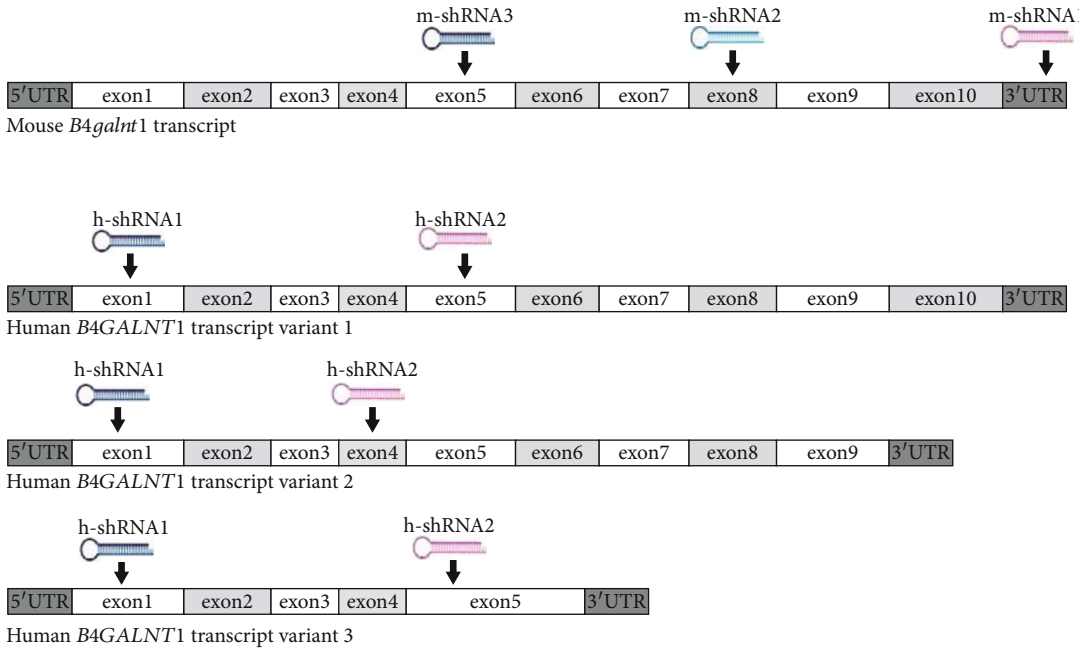

(c)

Figure 1: Ganglioside biosynthesis and degradation pathway in *Hexa*-/-*Neu3*-/- TSD model. The dotted lines indicate the knock-out genes and proposed silencing of the B4Galnt1 gene by shRNA treatment (a). Schematic presentation of self-complementary recombinant AAV vector including shRNA silencing cassettes controlled by U6 promoter and mCherry reporter gene regulated by CMV promoter (b). Location of the target regions of the shRNA(s) for mouse and human B4Galnt1 gene (c).

and 22 s at 72°C. The values were read after each cycle. Samples were compared against a standard curve of AAV plasmid diluted from 1×10^3 to 1×10^7 copies per milliliter. The vector genomes per milliliter were calculated via quantitative real-time PCR.

2.3. Cell Lines and Transduction Assay. Mouse fibroblasts were obtained from a skin biopsy of wild-type and *Hexa*-/-*Neu3*-/- mice at the age of 5 months. Human control and Tay-Sachs patient fibroblasts, obtained from forearm skin with a punch biopsy, were kindly donated by Dr. Nur Arslan, Child Neurology Department, Dokuz Eylül University. Mouse neuroglia cell (NG) cell line was generated from 100 mg brain tissue of 5-month-old wild-type and *Hexa*-/-*Neu3*-/- mice by using an adult brain dissociation kit according to manufacturer's instructions (Miltenyi Biotec, 130-107-677). After cell debris and red blood cell removal were performed, neurons were isolated by a neuron isolation kit according to the manufacturer's instructions (Miltenyi Biotec, 130-115-390). Primary cell lines were cultured in DMEM high glucose (Gibco) supplemented with 20% FBS (Gibco) and 1% (vol/vol) penicillin/streptomycin (Gibco) in a humidified incubator with 5% CO_2 at 37°C. Primary cell lines were infected with human papillomavirus (HPV) type 16 E6E7 (HPV16E6E7) retrovirus (ATCC® CRL-2203™), and uninfected primary cells were eliminated with 50 μg/ml of G418 (Sigma-Aldrich) for 14 days. The immortalized TSD neuroglia cells (Ng-125) obtained from the Tay-Sachs fetus were obtained [28]. TSD neuroglia cells producing active HEXA enzyme throughout cDNA clone of the α subunit of Hex A (pCMV-Hex α) were used as control of human neuroglia cells [29]. Immortalized cell lines were cultured in DMEM high glucose supplemented with 10% FBS and 1% (vol/vol) penicillin/streptomycin in a 37°C, 5% CO_2 incubator. Immortalized cell lines were seeded at 40–60% confluence. Cells were fed DMEM high glucose supplemented with 10% FBS with prior infection, media changed to 2% FBS, and cells were exposed to AAV9-B4Galnt1-shRNA for 1 hour. After that, a complete medium was added and incubation continued for up to 72 hours. All infections were performed with the same number of vg (6.0×10^9) for 3.6×10^5 cells. The transduction efficiency of each cell was measured based on mCherry signal, and the % of infected cells is presented in Figure S1.

2.4. Quantitative PCR Analysis. Total RNA was extracted from skin fibroblast and neuroglia cells derived from humans and mice by using TRIzol Reagent (Geneaid). RNA was then reverse transcribed into cDNA using iScript cDNA Synthesis Kit (BioRad). 50 ng RNA was used in each qRT-PCR reaction using iTaq Universal SYBR Green Supermix (BioRad) according to the manufacturer's instructions. The relative quantity of endogenous B4Galnt1 transcript in the cells had received the AAV9-B4Galnt1-shRNA compared with the cells that had no AAV9-B4Galnt1-shRNA. Primers in Table 1 were used in the qRT-PCR analysis. Each sample was run in triplicate, and relative concentration was calculated using the ddCt values normalized to endogenous GAPDH transcript.

2.5. Immunocytochemical Analysis. The cells treated with AAV9-B4Galnt1-shRNA were grown on micro slides on 24 well plates for 72 hours. The cells were fixed with 4%

Table 1: Primer sequences for the qRT-PCR analysis.

B4Galnt1	Mouse	F: 5′-GGGCGGTTGACCTCACTAAA-3′ R: 5′-GGAGAACCGGACTGTGTCTG-3′
B4GALNT1	Human	F: 5′-GGGCGGTTGACCTCACTAAA-3′ R: 5′-GGAGAACCGGACTGTGTCTG-3′
B3Galt4	Mouse	F: 5′-GGCAGTGCCCCTTCTGTATT-3′ R: 5′-GTGCAGTCCTCTCCCCATTC-3′
B3GALT4	Human	F: 5′-GGCAGTGCCCCTTCTGTATT-3′ R: 5′-GTGCAGTCCTCTCCCCATTC-3′
HexB	Mouse	F: 5′-AGTGCGAGTCCTTCCCTAGT-3′ R: 5′-ATCCGGACATCGTTTGGTGT-3′
HEXB	Human	F: 5′-AGTGCGAGTCCTTCCCTAGT-3′ R: 5′-ATCCGGACATCGTTTGGTGT-3′
Gm3s	Mouse	F: 5′-AATGCACTATGTGGACCCTG-3′ R: 5′-GTTGATGCTGTACCTGTCCTC-3′
GM3S	Human	F: 5′-AATGCACTATGTGGACCCTG-3′ R: 5′-GTTGATGCTGTACCTGTCCTC-3′
Gd3s	Mouse	F: 5′-CGATAATTCCACGTACTCCCTC-3′ R: 5′-TTTGGAACCGACATCTCTGG-3′
GD3S	Human	F: 5′-CGATAATTCCACGTACTCCCTC-3′ R: 5′-TTTGGAACCGACATCTCTGG-3′
Gapdh	Mouse	F: 5′-CCCCTTCATTGACCTCAACTAC-3′ R: 5′-ATGCATTGCTGACAATCTTGAG-3′
GAPDH	Human	F: 5′-CCCCTTCATTGACCTCAACTAC-3′ R: 5′-ATGCATTGCTGACAATCTTGAG-3′

paraformaldehyde for 30 min and incubated in a blocking solution (10% goat serum, 4%BSA 0.3 M Glycine, and 0.3% TritonX in 1XPBS) for 1 hour. The cells were stained with the primary antibodies (anti-GM2 1 : 250, anti-LAMP1: 1 : 250 "ab24170") and secondary antibodies (1 : 250, SA5-10118 Alexa Fluor®-488 and 1 : 500 ab150077, Alexa Fluor®-488), and they were mounted on slides with Fluoroshield mounting medium DAPI (Abcam). Immunocytochemical analysis was performed as $n = 3$ separate experiments, and 10 to 20 images were taken for each experiment. Images were obtained by using a fluorescent microscope (Olympus BX53), and intensity analysis of fluorescence was applied by using NIH ImageJ (Fiji).

3. Results

3.1. Quantitative PCR Analysis in Hexa-/-Neu3-/- Mouse Neuroglia and Fibroblast. Three different shRNAs designed for mouse *B4Galnt1* significantly silenced *B4Galnt1* gene expression. Quantitative PCR analyses demonstrated that the level of *B4Galnt1* mRNA in the AAV9-shRNA-transduced fibroblast was decreased by 64% for shRNA1 ($^{***}P < 0.005$), 45% for shRNA2 ($^{**}P < 0.01$), and 46% for shRNA3 ($^{**}P < 0.01$) when compared to the untreated cells (Figure 2(a)). Ganglioside biosynthesis/degradation pathway genes such as *B3Galt4*, *HexB*, *GM3S*, and *GD3S* were analyzed after AAV9-mshRNA-1 vector transduction to determine whether shRNA transduction affects other enzymes in the pathway. Although AAV9-m-shRNA1-transduced *Hexa-/-Neu3-/-* fibroblast showed significantly increased levels of *HexB* ($^{**}P < 0.01$) (Figure 2(c)) and *Gd3s* ($^{**}P < 0.01$) (Figure 2(e)) expression, the expression levels of the *B3Galt4* and *Gm3s* show no difference (Figures 2(b) and 2(d)).

We further analyzed the *Hexa-/-Neu3-/-* neuroglia and similar to the fibroblast, and m-shRNA1 was the most effective with 82% suppression of *B4Galnt1* ($^{**}P < 0.01$) while m-shRNA2 and m-shRNA3 suppressed the *B4Galnt1* expression by 38% ($^{*}P < 0.05$) and 67% ($^{*}P < 0.05$), respectively (Figure 2(f)). Although m-shRNA1 transduction does not affect *B3Galt4* (Figure 2(g)) and *HexB* (Figure 2(h)) gene expression, we observed significantly elevated levels of *Gm3s* ($^{***}P < 0.005$) (Figure 2(i)) and *Gd3S* ($^{*}P < 0.05$) (Figure 2(j)) expression in AAV9-mshRNA1-transduced *Hexa-/-Neu3-/-* neuroglia.

3.2. Quantitative PCR Analysis in TSD Fibroblast and Neuroglia Cells. Both shRNAs designed for human *B4GALNT1* significantly reduced the mRNA levels of *B4GALNT1*. AAV9-h-shRNA1 transduction reduced *B4GALNT1* more effectively than AAV9-h-shRNA2 in TSD fibroblast compared to untreated condition (60%; $^{***}P < 0.005$ versus 42%; $^{*}P < 0.05$, respectively) (Figure 3(a)). In TSD fibroblast, AAV9-h-shRNA1 transduction significantly increased *B3GALNT4* ($^{*}P < 0.05$) (Figure 3(b)), *GM3S* ($^{*}P < 0.05$) (Figure 3(d)), and *GD3S* ($^{*}P < 0.05$) (Figure 3(e)); however, *HEXB* expression level (Figure 3(c)) was not affected by shRNA transduction.

Additionally, AAV9-based knockdown of target gene expression in human neuroglia cells was more effective for h-shRNA1 (74%; $^{***}P < 0.005$) than h-shRNA2 (30%; $^{*}P < 0.05$) (Figure 3(f)). When we investigated the other genes in the ganglioside synthesis pathway, we found that expression levels of *HEXB* ($^{**}P < 0.01$) (Figure 3(h)), *GM3S* ($^{**}P < 0.01$) (Figure 3(i)), and *GD3S* ($^{*}P < 0.05$) (Figure 3(j)) were significantly increased in h-shRNA1-transduced TSD-Ng125 cells compared to untreated condition but not *B3GALT4* (Figure 3(g)).

3.3. Lysosomal Accumulation Is Reduced in TSD Mouse Fibroblast and Neuroglia Cells. Here, we examined the effects of AAV9-m-shRNA1 transduction on the lysosomal accumulation of GM2 ganglioside in the TSD mouse fibroblast and neuroglia. In untreated conditions, significantly increased GM2 (Figures 4(a), 4(b), and 4(d)) and Lamp1 accumulation (Figures 4(e), 4(f), and 4(h)) were shown in TSD mouse fibroblast compared to untreated control cells (Figures 4(d) and 4(h)). We demonstrated that *in vitro* knockdown of *B4Galnt1* by AAV9-m-shRNA1 significantly reduced GM2 ganglioside (Figures 4(c) and 4(d)) and lysosomal mass concentrations (Figures 4(g) and 4(h)) in the TSD mouse fibroblast compared to untreated cells (threefold, $^{**}P < 0.01$ versus twofold, $^{**}P < 0.01$, respectively) (Figures 4(d) and 4(h)).

Similar to the TSD mouse fibroblast cell line, TSD mouse neuroglia exhibited significantly increased accumulation of GM2 (Figures 5(a), 5(b), and 5(d)) and Lamp1

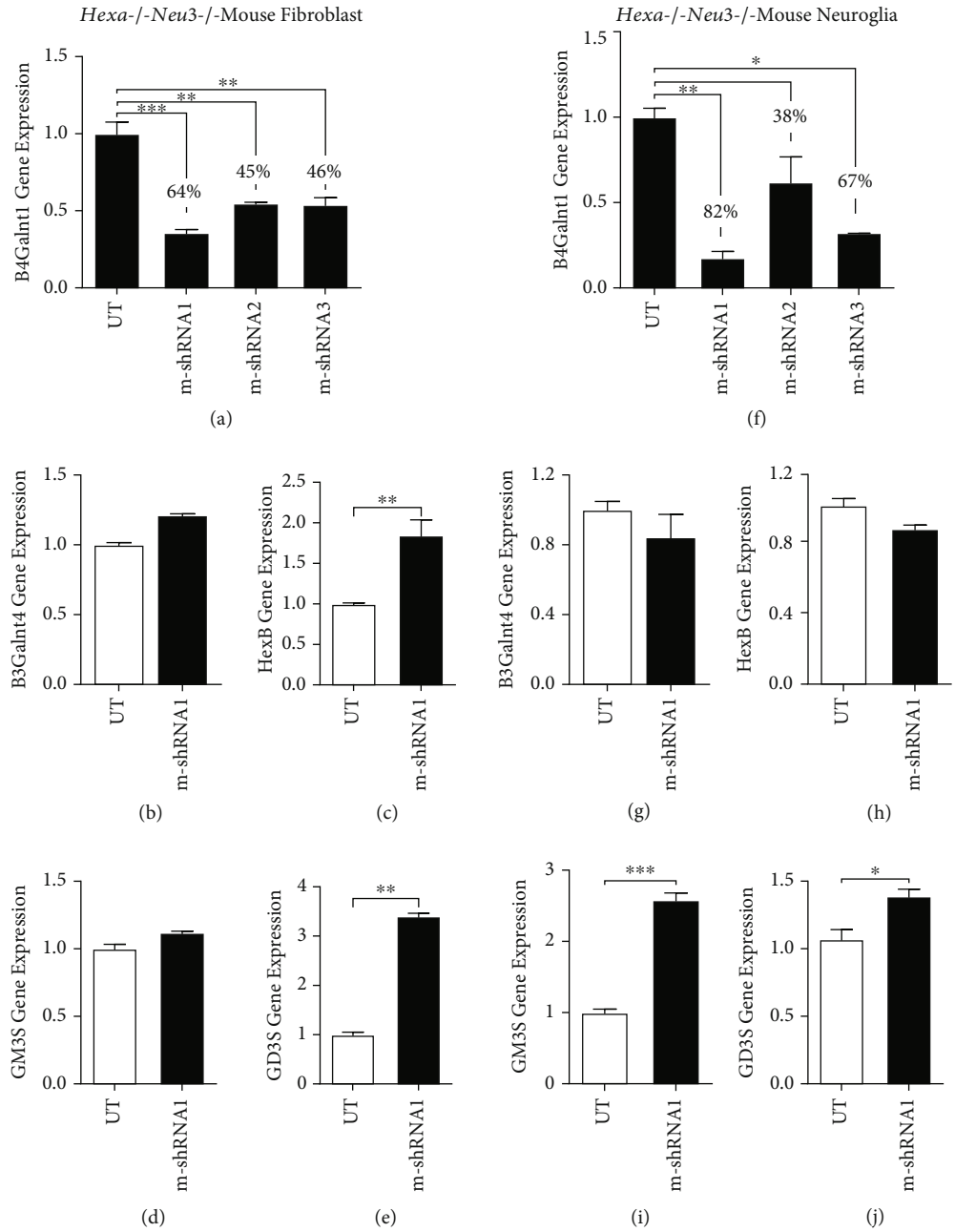

Figure 2: Gene expression analysis in (a–e) *Hexa-/-Neu3-/-* mouse fibroblast and (f–j) neuroglia. Evaluation of knockdown efficiency of B4Galnt1-m-shRNAs (m-shRNA1, m-shRNA2, and m-shRNA3) by qRT-PCR analysis at 72 hours post-transduction in (a) *Hexa-/-Neu3-/-* mouse fibroblast and (f) neuroglia. Relative expression levels of (b, g) B3Galnt4, (c, h) HexB, (d, i) Gm3s, and (e, j) Gd3s in untransduced and AAV9-m-shRNA1-transduced *Hexa-/-Neu3-/-* fibroblast and neuroglia, respectively ($n = 3$; $^{*}P < 0.05$, $^{**}P < 0.01$, and $^{***}P < 0.005$).

(Figures 5(e), 5(f), and 5(h)) when compared to untreated control cells (Figures 5(d) and 5(h)). Additionally, AAV9-mediated delivery of m-shRNA1 to the TSD mouse neuroglia demonstrated that AAV9 m-shRNA1 diminished the twofold GM2 ganglioside accumulation ($^{**}P < 0.01$) (Figures 5(c) and 5(d)) and lysosomal mass ($^{*}P < 0.05$) (Figures 5(g) and 5(h)). Altogether, our results proved that *B4Galnt1* silencing can potentially reduce lysosomal accumulation *in vitro* models of the Tay-Sachs disease mouse fibroblast and neuroglia cell line.

3.4. B4Galnt1 Silencing Reverses Lysosomal Pathology in TSD Patient Fibroblast and Neuroglia. GM2 ganglioside accumulation causes enlargement of the lysosomes and LAMP1 accumulation at the cellular level [30]. Similar to mouse cells, significantly increased GM2 (Figures 6(a), 6(b), and 6(d)) and Lamp1 (Figures 6(e), 6(f), and 6(h)) accumulation was demonstrated in TSD human fibroblast when compared to untreated control cells. In addition, neuroglia (Figures 7(d) and 7(h)) cell lines from TSD patients displayed significantly increased GM2 (Figures 7(a), 7(b), and 7(d)) and Lamp1

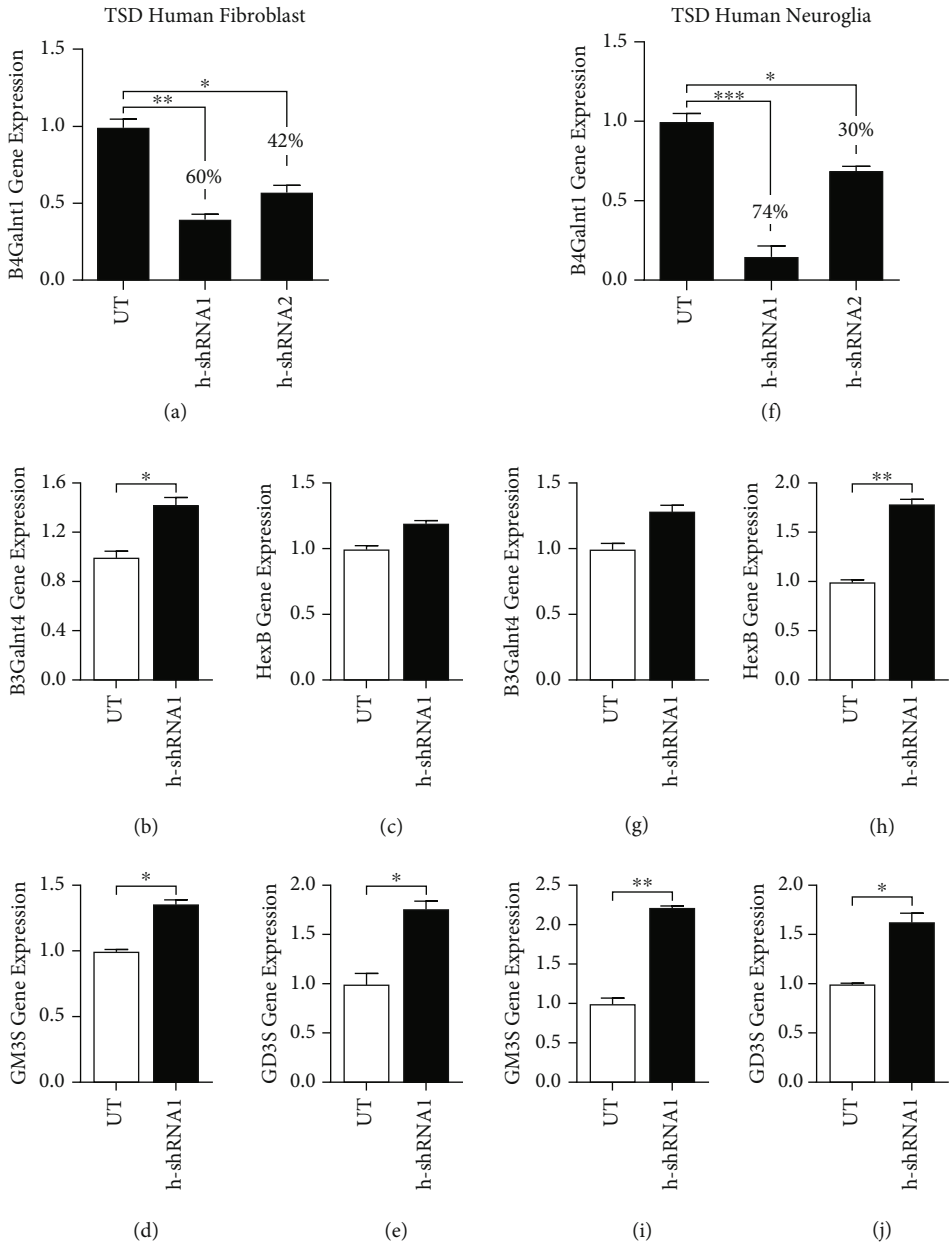

Figure 3: Gene expression analysis in (a–e) TSD human fibroblast and (f–j) neuroglia. Evaluation of knockdown efficiency of B4Galnt1-m-shRNAs (h-shRNA1 and h-shRNA2) by qRT-PCR analysis at 72 hours post-transduction in (a) TSD human fibroblast and (f) neuroglia. Relative expression levels of (b, g) B3GALT4, (c, h) HEXB, (d, i) GM3S, and (e, j) GD3S in untransduced and AAV9-h-shRNA1-transduced TSD human fibroblast and neuroglia, respectively ($n = 3$; $^{*}P < 0.05$, $^{**}P < 0.01$, and $^{***}P < 0.005$).

(Figures 7(e), 7(f), and 7(h)) accumulation. We examined the effects of AAV9-h-shRNA1 transduction on the GM2 (Figures 6(c) and 6(d)) and Lamp1 (Figures 6(g) and 6(h)) accumulation observed on TSD patient fibroblast. Similar to TSD patient fibroblast, we also studied the effects of AAV9-h-shRNA1 transduction on the GM2 (Figures 7(c) and 7(d)) and Lamp1 (Figures 7(g) and 7(h)) accumulation. Silencing the *B4GALNT1* gene reduced approximately five-fold GM2 ganglioside intensity ($^{*}P < 0.05$) in the TSD patient fibroblast (Figure 6(d)). Moreover, LAMP1 intensity also was improved threefold ($^{****}P < 0.001$) after AAV9-h-shRNA1 transduction compared to untreated TSD patient fibroblast (Figure 6(h)).

We further displayed AAV9-h-shRNA1 transduction in the TSD neuroglia cell line. Immunofluorescence staining of the GM2 and LAMP1 demonstrated that the knockdown of *B4GALNT1* by AAV9-h-shRNA1 significantly reduced the lysosomal accumulation of the GM2 ganglioside ($^{**}P < 0.001$) (Figure 7(d)) and a lysosomal marker of LAMP1 ($^{*}P < 0.05$) in TSD patient neuroglia cell (Figure 7(h)).

4. Discussion

The Tay-Sachs disease is a neurodegenerative lysosomal storage disorder resulting from genetic mutations in the HEXA gene leading to the accumulation of GM2 ganglioside

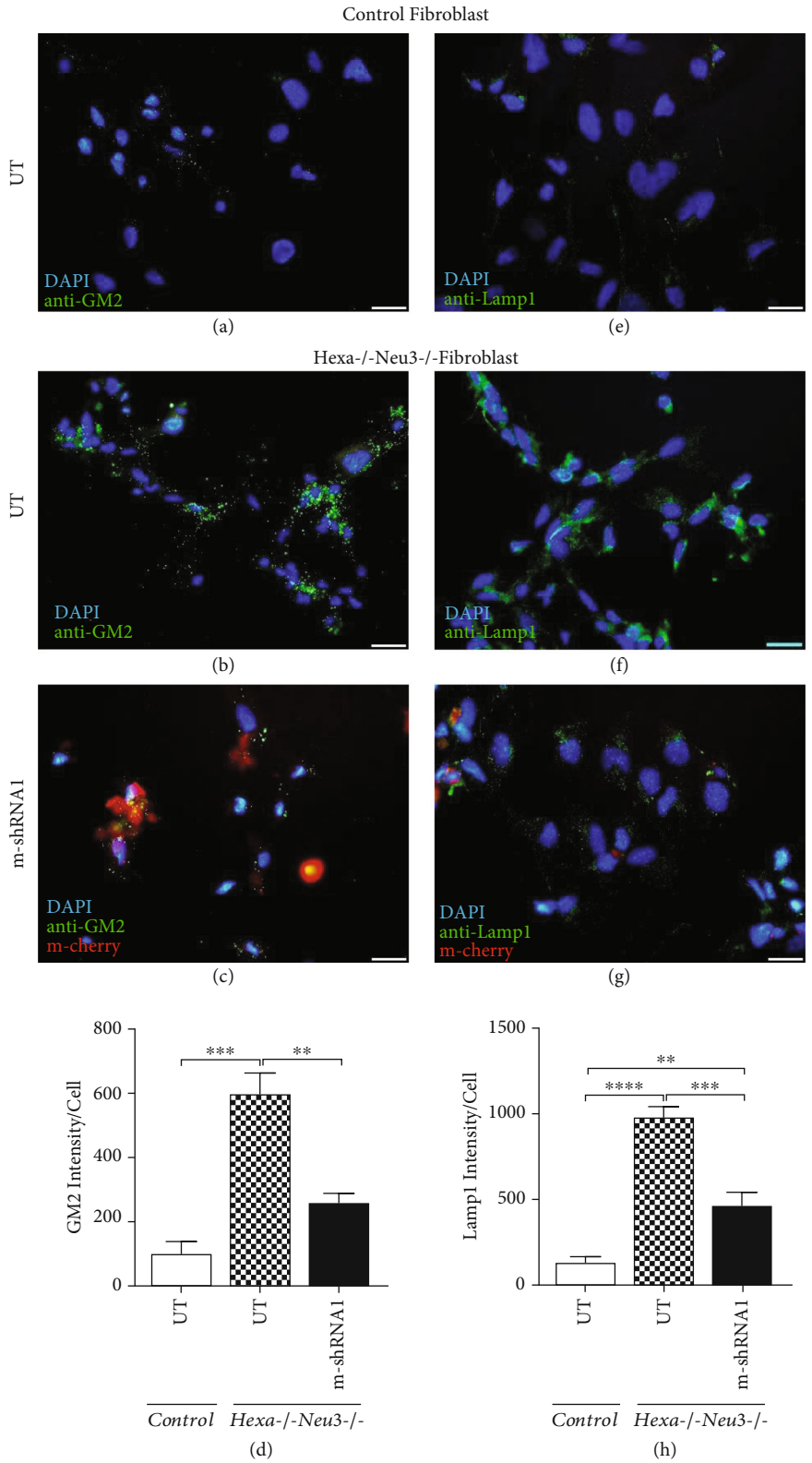

FIGURE 4: Immunocytochemical analysis of GM2 and Lamp1 in control and *Hexa-/-Neu3-/-* mouse fibroblast. *Hexa-/-Neu3-/-* mouse fibroblast was transduced with 6×10^9 viral particles of AAV9-h-shRNA1 expressing mCherry reporter gene (red) in 24-well plates. Representative fluorescent images showed (a–c) GM2 ganglioside and (e–g) lysosome levels in the untreated and AAV9-transduced cells stained with anti-GM2 (green) and anti-Lamp1 (green) antibodies following 72 hours post-transduction. The total intensity of fluorescence was quantified using Fiji imaging software. Graphical representations were indicated for (d) GM2 and (h) Lamp1 intensity per cell ($n = 3$; $^{**}P < 0.01$, $^{***}P < 0.005$, and $^{****}P < 0.001$; scale bar represents 100 μm).

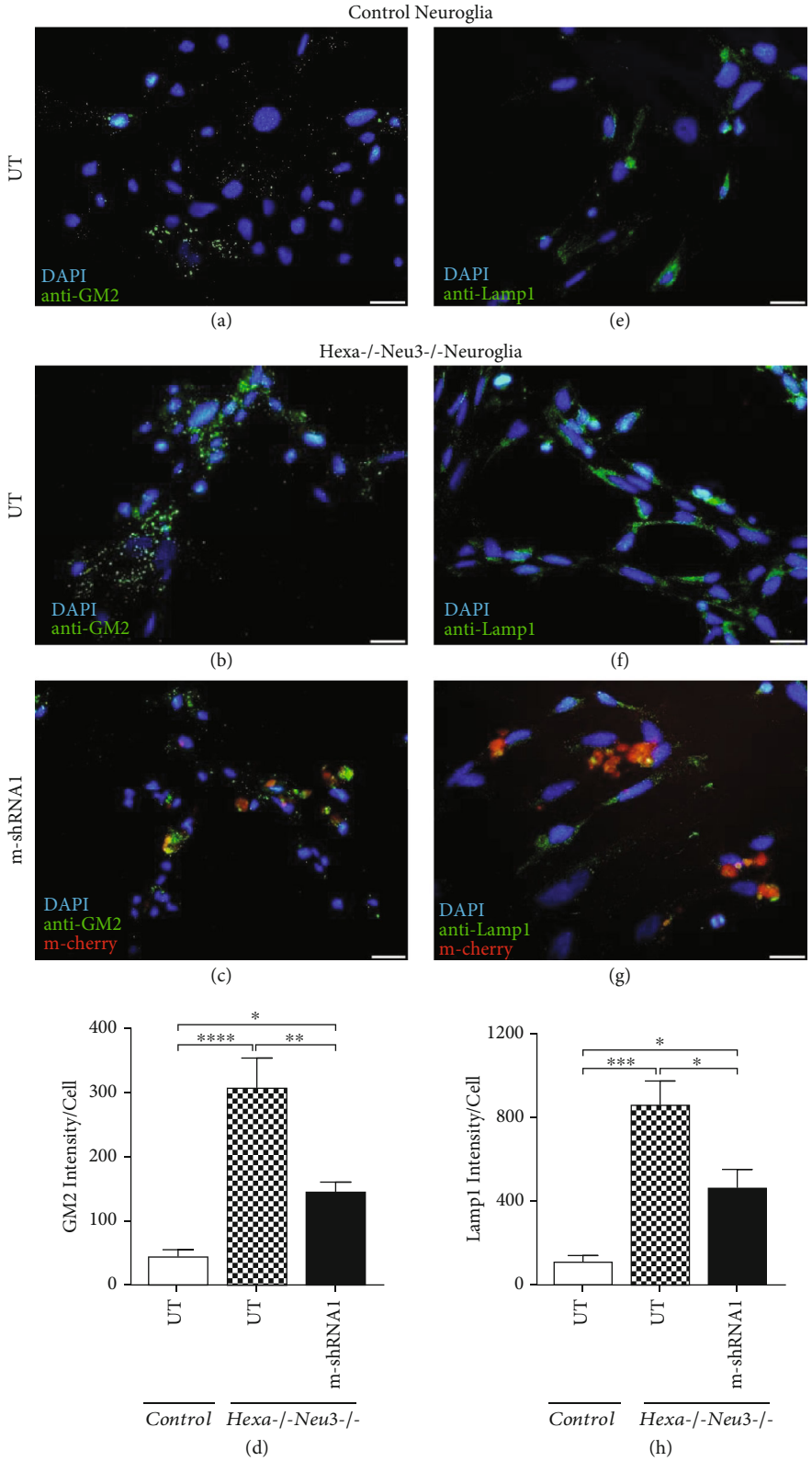

FIGURE 5: Immunocytochemical analysis of GM2 and Lamp1 in control and *Hexa-/-Neu3-/-* mouse neuroglia. *Hexa-/-Neu3-/-* mouse neuroglia was transduced with 6×10^9 viral particles of AAV9-h-shRNA1 expressing mCherry reporter gene (red) in 24-well plates. Representative fluorescent images showed (a–c) GM2 ganglioside and (e–g) lysosome levels in the untreated and AAV9-transduced cells with anti-GM2 (green) and anti-Lamp1 (green) antibodies following 72 hours post-transduction. The total intensity of fluorescence was quantified using Fiji imaging software. Graphical representations were indicated for (d) GM2 and (h) Lamp1 intensity per cell ($n = 3$; $^*P < 0.05$, $^{**}P < 0.01$, $^{***}P < 0.005$, and $^{****}P < 0.001$; scale bar represents 100 μm).

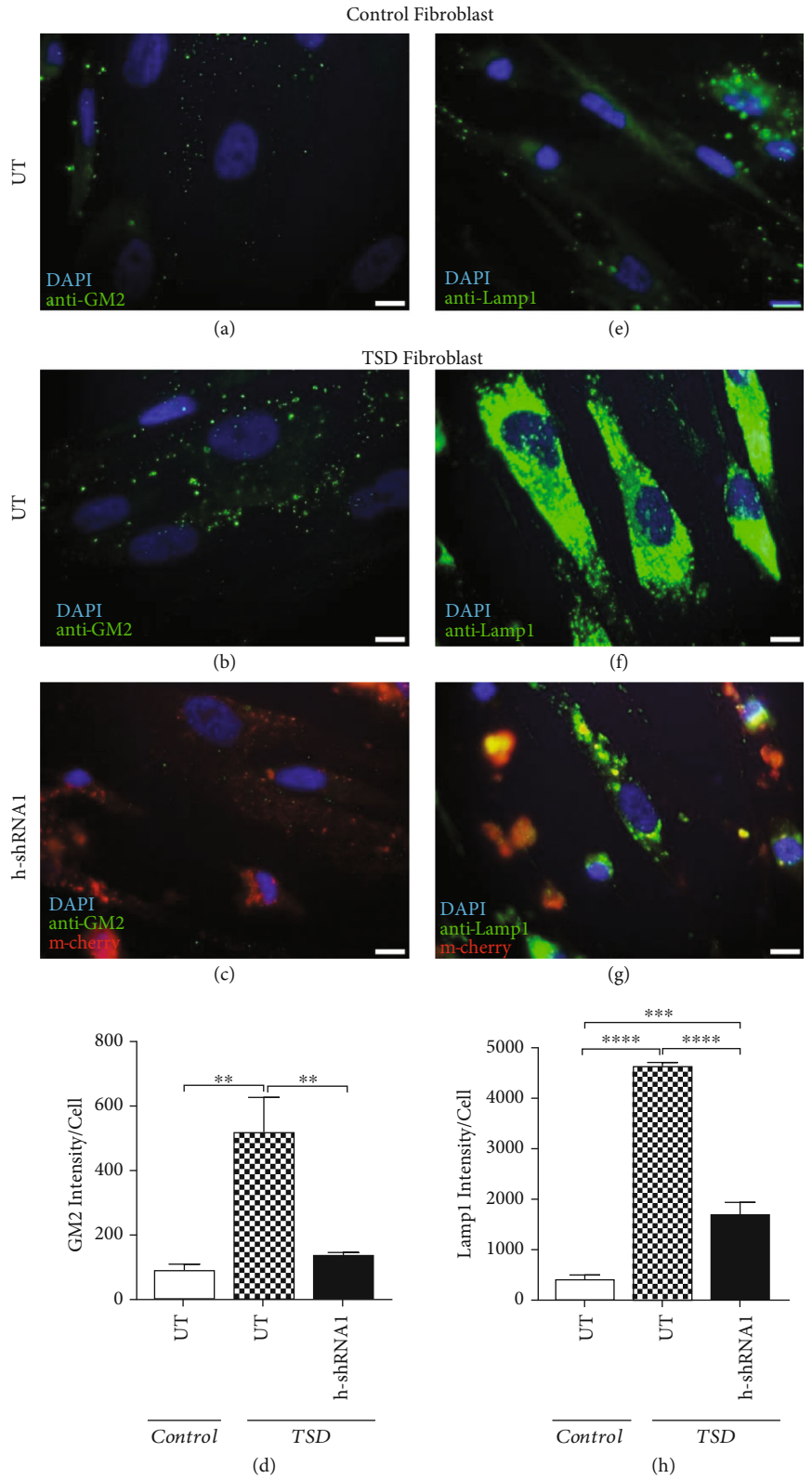

FIGURE 6: Immunocytochemical analysis of GM2 and Lamp1 in control and TSD human fibroblast. TSD human fibroblasts were transduced with 6×10^9 viral particles of AAV9-h-shRNA1 expressing mCherry reporter gene (red) in 24-well plates. Representative fluorescent images showed (a) GM2 ganglioside and (b) lysosome levels in the *uninfected* and AAV9-infected cells with anti-GM2 (green) and anti-Lamp1 (green) antibodies following 72 hours post-transduction. The total intensity of fluorescence was quantified using Fiji imaging software ($n = 3$; $^{*}P < 0.05$, $^{**}P < 0.01$, $^{***}P < 0.005$, and $^{****}P < 0.001$; scale bar represents 100 μm).

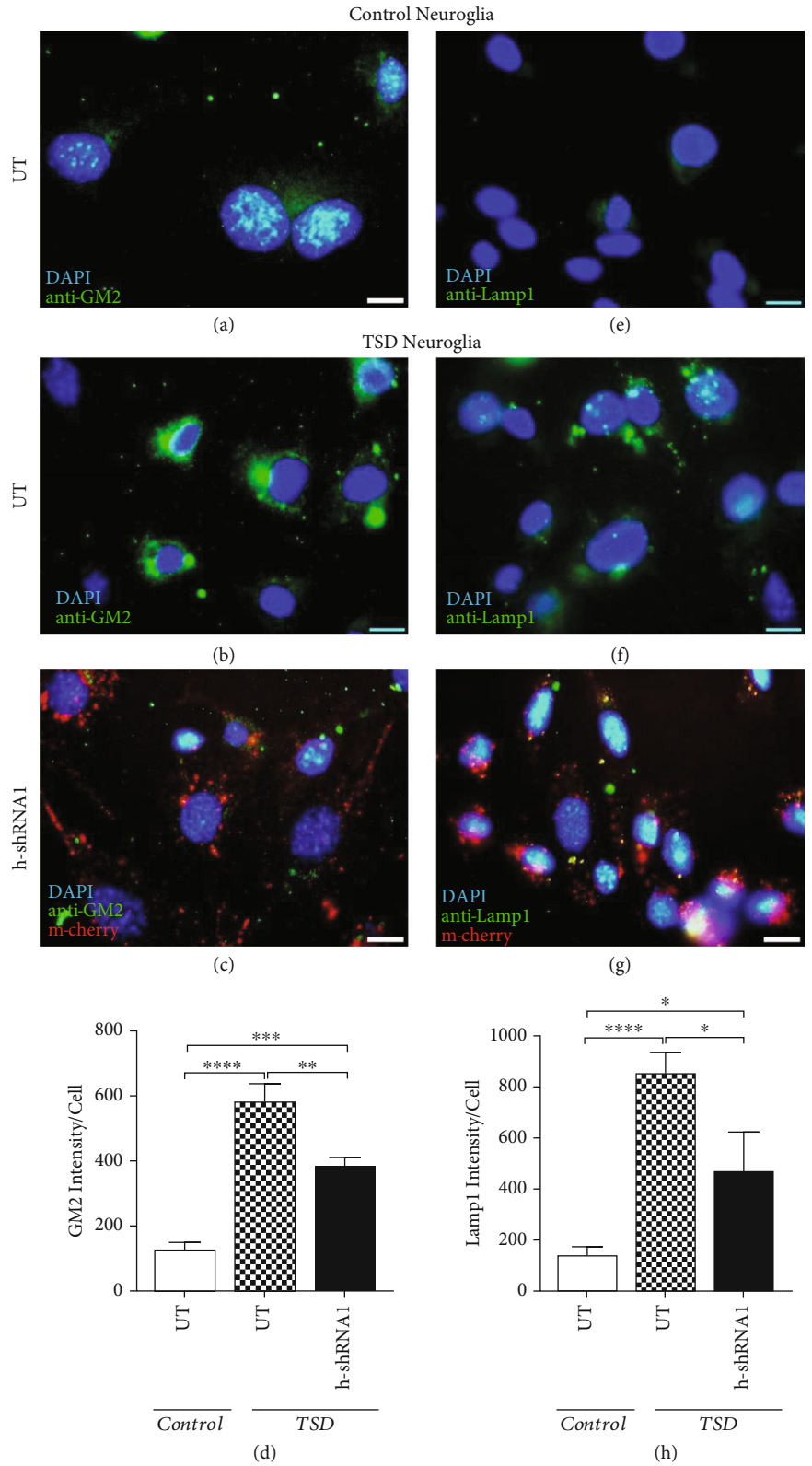

FIGURE 7: Immunocytochemical analysis of GM2 and Lamp1 in control and TSD human neuroglia. TSD human neuroglia was transduced with 6×10^9 viral particles of AAV9-h-shRNA1 expressing mCherry reporter gene (red) in 24-well plates. Representative fluorescent images showed (a–c) GM2 ganglioside and (e–g) lysosome levels in the untreated and AAV9-transduced cells with anti-GM2 (green) and anti-Lamp1 (green) antibodies following 72 hours post-transduction. The total intensity of fluorescence was quantified using Fiji imaging software. Graphical representations were indicated for (d) GM2 and (h) Lamp1 intensity per cell ($n = 3$; $^{*}P < 0.05$, $^{**}P < 0.01$, $^{***}P < 0.005$, and $^{****}P < 0.001$; scale bar represents 100 μm).

in the CNS. There is no effective treatment for patients with Tay-Sachs yet. Enzyme replacement therapy, stem cell transplantation, substrate reduction therapy, or gene therapy comprises the main treatment strategies for many lysosomal storage disorders [31]. Some of them provide or enhance the activity of the missing enzyme to re-establish substrate catabolism; however, others have no impact on the correction of neuropathology for diseases like Tay-Sachs because of the blood-brain barrier. Viral vector-based gene therapies are one of the novel treatment strategies for lysosomal storage disorders to provide the activity of the missing enzyme and re-establish substrate metabolism in the CNS [32]. A bunch of studies have shown the potential for AAV treatment in the management of gangliosidosis models *in vitro* and *in vivo* [17, 33–35]. In the present study, we suggest a new experimental treatment strategy for the Tay-Sachs disease using AAV-mediated RNAi technology targeting the human and mouse B4Galnt1 gene which catalyzes GM2 biosynthesis.

Substrate reduction therapy (SRT) acts upstream of the enzymatic defect, decreasing storage by silencing its biosynthetic pathway. β-1,4-N–Acetylgalactosaminyl transferase coded by the B4Galnt1 gene is a key enzyme in the ganglioside biosynthesis pathway involving the conversion of GM3 to GM2 [9]. In our study, we selected the B4Galnt1 gene as a target for substrate reduction therapy to decrease GM2 biosynthesis and eventually its accumulation in cell models of the Tay-Sachs disease. Deficiency of the B4GALNT1 enzyme in mice leads to the complete absence of major brain gangliosides; instead, the less complex gangliosides GM3 and GD3 are found in higher concentrations since they are synthesized before the block in the biosynthetic pathway. Interestingly, despite the lack of complex ganglioside biosynthesis, the overall levels of glycosphingolipids (GSLs) in the *B4Galnt1* KO mice remain comparable to those in normal mice due to the compensatory increase in the upstream synthesis of simple GSLs [36]. Gangliosides play multifaceted roles especially during the neurodevelopmental stage, contributing to the important processes that shape the developing nervous system [37]. Their involvement in neuronal migration, axon guidance, dendritic arborization, synaptogenesis, and myelination highlights their significance in ensuring proper neuronal development and function [38]. Simple gangliosides, such as GM3, are prevalent during early neurodevelopmental stages and are involved in fundamental processes like cell proliferation, migration, and differentiation. As neurodevelopment progresses, there is a shift towards expressing more complex gangliosides, like GD1a, GD1b, and GT1b. These complex gangliosides are enriched in mature neurons and are intricately involved in synaptic plasticity, neurotransmitter release, and signal transduction [39]. The balance between simple and complex gangliosides is tightly regulated throughout neurodevelopment, ensuring proper neuronal maturation and function. Dysregulation of ganglioside metabolism or expression has been implicated in various neurodevelopmental disorders, including intellectual disabilities, developmental delay, and neurological disorders like hereditary spastic paraplegia (HSP) [40]. In humans, mutations in the *B4GALNT1* gene have been shown to cause HSP which is a genetically heterogeneous group of neurological disorders characterized clinically by slow progressive lower limb spasticity and the axonal degeneration in the corticospinal tracts [41]. It has been reported that mutations on *B4GALNT1* that cause loss of function of the enzyme lead to HSP with an extreme phenotype, with very limited exceptions that reduced enzyme activity (M4 mutant) causes a mild phenotype of HSP disease. Additionally, an 85% reduction of the B4GALNT1 enzyme activity is caused by the read through of the nonsense mutation at codon 228 of the *B4GALNT1* gene which alleviates the clinical pathology of HSP patients [42]. We suggest that silencing the *B4GALNT1* gene at the postnatal stage in TSD patients may prevent the neurodevelopmental abnormalities observed in HSP patients with B4GALNT1 deficiency. Here, we first aimed to determine the effectiveness of silencing *B4GALNT1* by AAV-mediated-shRNA treatment *in vitro* and address the basis for future studies *in vivo* to treat the TSD mouse model we generated.

In the present study, we first prepared the shRNAs with AAV9 which is an efficient natural AAV serotype bypassing the BBB and efficiently targeting cells of the CNS [19, 43]. In our *in vitro* study, therefore, we transduced both mouse and human TSD fibroblast and neuroglia with rAAV9-B4Galnt1-shRNAs and determined m-shRNA1 and h-shRNA1 as the most efficient siRNAs in mouse and human cells, respectively.

We demonstrated that although silencing of *B4galnt1* with m-shRNA1 and h-shRNA1 displayed an increasing pattern for B3GALT4 gene expression, it was statistically not significant. We speculate that this situation might be related to accumulated GM2 ganglioside amounts in each cell type where B3GALT4 catalyzes GM2 to GM1 conversion; however, this hypothesis requires further investigation.

Previously, it has been demonstrated that B4GALNT1 deficiency leads to increased synthesis of GM3 and GD3 gangliosides in human fibroblast and mouse models, as B4GALNT1 is at the downstream of GM3 synthesis in the ganglioside synthesis pathway [44, 45]. Consistently, our data showed significantly increased levels of GM3S expression in all cell models except mouse fibroblast. Elevated levels of GD3S expression in all cell models studied also suggest a higher rate of GM3 biosynthesis when B4GALNT1 is silenced. Additionally, significantly increased HexB gene expression levels in mouse fibroblast and human neuroglia might be related to the compensation mechanisms due to GSL alterations under the same conditions. Our immunocytochemical data using anti-GM2 and anti-LAMP1 also displayed silencing of the *B4GALNT1* gene enabling the depletion of accumulated GM2 and lysosomal mass in both human and mouse TSD cell models.

Overall, we suggest a new strategy for the treatment of TSD with the proof concept of study using AAV-mediated RNAi technology targeting the *B4GALNT1* gene at the upstream of the enzymatic defect in TSD pathology. We demonstrated that AAV9-B4Galnt1-shRNA transduction could effectively suppress B4GALNT1 expression and reverse lysosomal storage of GM2 ganglioside in both mouse and human TSD cell models. Therefore, we address that

silencing of *B4GALNT1* might provide the basic knowledge that could be applied to treat the novel mouse model of TSD, *Hexa-/-Neu3-/-* which we recently generated and potentially for the treatment of TSD patients in the future.

Data Availability

The all data used to support the findings of this study are included within the article.

Conflicts of Interest

The authors declare that the research was conducted without any commercial or financial relationships that could be construed as a potential conflict of interest.

Acknowledgments

This study was funded by the Scientific and Technological Research Council of Turkey (TUBITAK) (Project No. 218S824). NA and OKI were supported by the Turkish Higher Education Council's 100/2000 Ph.D. Fellowship Program and the TUBITAK BIDEB National Scholarship Program for Ph.D. students (2211-A).

Supplementary Materials

Figure S1: immunocytochemical analysis of transfection efficiency of m-shRNA1 in *Hexa-/-Neu3-/-* mouse fibroblast, *Hexa-/-Neu3-/-* mouse neuroglia, TSD human fibroblast, and TSD human neuroglia. Cells in 24-well plates were infected with 6×10^9 viral particles of AAV9-m-shRNA1 expressing the mCherry reporter gene (red). The intensity of fluorescence was quantified using Fiji imaging software, and the percent of transduced cells 72 hours post-transduction was calculated ($n = 3$; scale bar represents 100 μm). *(Supplementary Materials)*

References

[1] K. Sandhoff and K. Harzer, "Gangliosides and gangliosidoses: Principles of molecular and metabolic pathogenesis," *Journal of Neuroscience*, vol. 33, no. 25, pp. 10195–10208, 2013.

[2] A. F. Leal, E. Benincore-Flórez, D. Solano-Galarza et al., "Gm2 gangliosidoses: clinical features, pathophysiological aspects, and current therapies," *International Journal of Molecular Sciences*, vol. 21, no. 17, 2020.

[3] K. Sango, S. Yamanaka, A. Hoffmann et al., "Mouse models of Tay-Sachs and Sandhoff diseases differ in neurologic phenotype and ganglioside metabolism," *Nature Genetics*, vol. 11, no. 2, pp. 170–176, 1995.

[4] J. A. Yuziuk, C. Bertoni, T. Beccari et al., "Specificity of mouse GM2 activator protein and β-N-acetylhexosaminidases A and B," *Journal of Biological Chemistry*, vol. 273, no. 1, pp. 66–72, 1998.

[5] V. Seyrantepe, S. A. Demir, Z. K. Timur et al., "Murine Sialidase Neu3 facilitates GM2 degradation and bypass in mouse model of Tay-Sachs disease," *Experimental Neurology*, vol. 299, no. Part A, pp. 26–41, 2018.

[6] S. A. Demir, Z. K. Timur, N. Ateş, L. A. Martínez, and V. Seyrantepe, "GM2 ganglioside accumulation causes neuroinflammation and behavioral alterations in a mouse model of early onset Tay-Sachs disease," *Journal of Neuroinflammation*, vol. 17, no. 1, 2020.

[7] R. Sandhoff and K. Sandhoff, "Emerging concepts of ganglioside metabolism," *FEBS Letters*, vol. 592, no. 23, pp. 3835–3864, 2018.

[8] S. Sipione, J. Monyror, D. Galleguillos, N. Steinberg, and V. Kadam, "Gangliosides in the brain: physiology, pathophysiology and therapeutic applications," *Frontiers in Neuroscience*, vol. 14, article 572965, 2020.

[9] K. Furukawa, K. Takamiya, and K. Furukawa, "β1,4-N-acetylgalactosaminyltransferase - GM2/GD2 synthase: a key enzyme to control the synthesis of brain-enriched complex gangliosides," *Biochimica et Biophysica Acta (BBA)-General Subjects*, vol. 1573, no. 3, pp. 356–362, 2002.

[10] E. M. Novelli and J. A. Barranger, "Gene therapy for lysosomal storage disorders," *Expert Opinion on Biological Therapy*, vol. 1, no. 5, pp. 857–867, 2001.

[11] M. B. Cachon-Gonzalez, E. Zaccariotto, and T. M. Cox, "Genetics and therapies for GM2 gangliosidosis," *Current Gene Therapy*, vol. 18, no. 2, pp. 68–89, 2018.

[12] M. S. Sands and M. E. Haskins, "CNS-directed gene therapy for lysosomal storage diseases," *Acta Paediatrica*, vol. 97, no. 457, pp. 22–27, 2008.

[13] D. Wang, P. W. L. Tai, and G. Gao, "Adeno-associated virus vector as a platform for gene therapy delivery," *Nature Reviews Drug Discovery*, vol. 18, no. 5, pp. 358–378, 2019.

[14] C. Roca, S. Motas, S. Marco et al., "Disease correction by AAV-mediated gene therapy in a new mouse model of mucopolysaccharidosis type IIID," *Human Molecular Genetics*, vol. 26, no. 8, pp. 1535–1551, 2017.

[15] S. M. Salabarria, J. Nair, N. Clement et al., "Advancements in AAV-mediated gene therapy for Pompe disease," *Journal of Neuromuscular Diseases*, vol. 7, no. 1, pp. 15–31, 2020.

[16] Y. Kurokawa, H. Osaka, T. Kouga et al., "Gene therapy in a mouse model of Niemann-Pick disease type C1," *Human Gene Therapy*, vol. 32, no. 11-12, pp. 589–598, 2021.

[17] R. C. Baek, M. L. D. Boekman, S. G. Leroy et al., "AAV-mediated gene delivery in adult GM1-gangliosidosis mice corrects lysosomal storage in CNS and improves survival," *PLoS One*, vol. 5, no. 10, 2010.

[18] A. M. Bradbury, T. A. Peterson, A. L. Gross et al., "AAV-mediated gene delivery attenuates neuroinflammation in feline Sandhoff disease," *Neuroscience*, vol. 340, pp. 117–125, 2017.

[19] K. D. Foust, E. Nurre, C. L. Montgomery, A. Hernandez, C. M. Chan, and B. K. Kaspar, "Intravascular AAV9 preferentially targets neonatal neurons and adult astrocytes," *Nature Biotechnology*, vol. 27, no. 1, pp. 59–65, 2009.

[20] H. Fu, J. Dirosario, S. Killedar, K. Zaraspe, and D. M. McCarty, "Correction of neurological disease of mucopolysaccharidosis IIIB in adult mice by rAAV9 trans-blood-brain barrier gene delivery," *Molecular Therapy*, vol. 19, no. 6, pp. 1025–1033, 2011.

[21] J. S. Walia, N. Altaleb, A. Bello et al., "Long-term correction of Sandhoff disease following intravenous delivery of rAAV9 to mouse neonates," *Molecular Therapy*, vol. 23, no. 3, pp. 414–422, 2015.

[22] C. M. Weismann, J. Ferreira, A. M. Keeler et al., "Systemic AAV9 gene transfer in adult GM1 gangliosidosis mice reduces lysosomal storage in CNS and extends lifespan," *Human Molecular Genetics*, vol. 24, no. 15, pp. 4353–4364, 2015.

[23] Y. L. Latour, R. Yoon, S. E. Thomas et al., "Human GLB1 knockout cerebral organoids: A model system for testing AAV9-mediated GLB1 gene therapy for reducing GM1 ganglioside storage in GM1 gangliosidosis," *Molecular Genetics and Metabolism Reports*, vol. 21, article 100513, 2019.

[24] S. Du, H. Ou, R. Cui et al., "Delivery of glucosylceramidase beta gene using AAV9 vector therapy as a treatment strategy in mouse models of Gaucher disease," *Human Gene Therapy*, vol. 30, no. 2, pp. 155–167, 2019.

[25] R. Martier and P. Konstantinova, "Gene therapy for neurodegenerative diseases: slowing down the ticking clock," *Frontiers in Neuroscience*, vol. 14, 2020.

[26] D. M. O'Connor and N. M. Boulis, "Gene therapy for neurodegenerative diseases," *Trends in Molecular Medicine*, vol. 21, no. 8, pp. 504–512, 2015.

[27] J. A. Picache, W. Zheng, and C. Z. Chen, "Therapeutic strategies for Tay-Sachs disease," *Frontiers in Pharmacology*, vol. 13, 2022.

[28] L. M. Hoffman, D. Amsterdam, and L. Schneck, "GM2∗ ganglioside in fetal Tay-Sachs disease brain cultures: a model system for the disease," *Brain Research*, vol. 111, no. 1, pp. 109–117, 1976.

[29] M. J. G. Fernandes, S. Yew, D. Leclerc et al., "Identification of candidate active site residues in lysosomal β-hexosaminidase A," *Journal of Biological Chemistry*, vol. 272, no. 2, pp. 814–820, 1997.

[30] D. A. Wenger, S. Coppola, and S. L. Liu, "Lysosomal storage disorders: diagnostic dilemmas and prospects for therapy," *Genetics in Medicine*, vol. 4, no. 6, pp. 412–419, 2002.

[31] M. Beck, "Treatment strategies for lysosomal storage disorders," *Developmental Medicine & Child Neurology*, vol. 60, no. 1, pp. 13–18, 2018.

[32] M. J. Edelmann and G. H. B. Maegawa, "CNS-targeting therapies for lysosomal storage diseases: current advances and challenges," *Frontiers in Molecular Biosciences*, vol. 7, 2020.

[33] M. L. D. Broekman, R. C. Baek, L. A. Comer, J. L. Fernandez, T. N. Seyfried, and M. Sena-Esteves, "Complete correction of enzymatic deficiency and neurochemistry in the GM1-gangliosidosis mouse brain by neonatal adeno-associated virus-mediated gene delivery," *Molecular Therapy*, vol. 15, no. 1, pp. 30–37, 2007.

[34] M. B. Cachón-González, S. Z. Wang, A. Lynch, R. Ziegler, S. H. Cheng, and T. M. Cox, "Effective gene therapy in an authentic model of Tay-Sachs-related diseases," *Proceedings of the National Academy of Sciences*, vol. 103, no. 27, pp. 10373–10378, 2006.

[35] T. J. Sargeant, S. Wang, J. Bradley et al., "Adeno-associated virus-mediated expression of β-hexosaminidase prevents neuronal loss in the Sandhoff mouse brain," *Human Molecular Genetics*, vol. 20, no. 22, pp. 4371–4380, 2011.

[36] K. Takamiya, A. Yamamoto, K. Furukawa et al., "Mice with disrupted GM2/GD2 synthase gene lack complex gangliosides but exhibit only subtle defects in their nervous system," *Proceedings of the National Academy of Sciences*, vol. 93, no. 20, pp. 10662–10667, 1996.

[37] K. Palmano, A. Rowan, R. Guillermo, J. Guan, and P. McJarrow, "The role of gangliosides in neurodevelopment," *Nutrients*, vol. 7, no. 5, pp. 3891–3913, 2015.

[38] J. F. Vasques, R. G. de Jesus Gonçalves, A. J. da Silva-Junior, R. S. Martins, F. Gubert, and R. Mendez-Otero, "Gangliosides in nervous system development, regeneration, and pathologies," *Neural Regeneration Research*, vol. 18, no. 1, pp. 81–86, 2023.

[39] R. K. Yu, Y. T. Tsai, and T. Ariga, "Functional roles of gangliosides in neurodevelopment: an overview of recent advances," *Neurochemical Research*, vol. 37, no. 6, pp. 1230–1244, 2012.

[40] L. E. O. Elsayed, I. Z. Eltazi, A. E. Ahmed, and G. Stevanin, "Insights into clinical, genetic, and pathological aspects of hereditary spastic paraplegias: a comprehensive overview," *Frontiers in Molecular Biosciences*, vol. 8, article 690899, 2021.

[41] A. Boukhris, R. Schule, J. L. Loureiro et al., "Alteration of ganglioside biosynthesis responsible for complex hereditary spastic paraplegia," *The American Journal of Human Genetics*, vol. 93, no. 1, pp. 118–123, 2013.

[42] R. H. Bhuiyan, Y. Ohmi, Y. Ohkawa et al., "Loss of enzyme activity in mutated B4GALNT1 gene products in patients with hereditary spastic paraplegia results in relatively mild neurological disorders: similarity with phenotypes of *B4galnt1* knockout mice," *Neuroscience*, vol. 397, pp. 94–106, 2019.

[43] R. D. Dayton, D. B. Wang, and R. L. Klein, "The advent of AAV9 expands applications for brain and spinal cord gene delivery," *Expert Opinion on Biological Therapy*, vol. 12, no. 6, pp. 757–766, 2012.

[44] G. V. Harlalka, A. Lehman, B. Chioza et al., "Mutations in *B4GALNT1* (GM2 synthase) underlie a new disorder of ganglioside biosynthesis," *Brain*, vol. 136, no. 12, pp. 3618–3624, 2013.

[45] H. Kawai, M. L. Allende, R. Wada et al., "Mice expressing only monosialoganglioside GM3 exhibit lethal audiogenic seizures," *Journal of Biological Chemistry*, vol. 276, no. 10, pp. 6885–6888, 2001.